Correlation of Chemical Composition and Microstructure with Properties of Poly(ε-caprolactone-*co-p*-dioxanone) Random Copolymers

Tianqiang Wang, Huizhen Zhao, Yu Liu, Jianyuan Hao

State Key Lab of Electronic Films and Integrated Devices, School of Microelectronics and Solid State Electronics, University of Electronic Science and Technology of China, Chengdu 610054, Sichuan, People's Republic of China
Correspondence to: J. Hao (E-mail: jyhao@uestc.edu.cn)

ABSTRACT: With the aim to develop novel biodegradable materials with good flexibility and fast degradation rate, random copolymers of ε-caprolactone (CL) and *p*-dioxanone (PDO) with a full range of compositions were synthesized in bulk using stannous octoate as the ring-opening catalyst. The chemical composition and number average sequence lengths of CL and PDO units determined by ^{1}H-NMR were used to correlate with various properties of the copolymers. Although both CL and PDO are crystalline components, only one crystalline phase could be present for each copolymer. The low limit of average block length for the copolymers that could crystallize is 3.22 for L_{CL} and 3.43 for L_{PDO}, respectively. The crystallinity and crystalline morphology of the copolymers are dependent on the crystalline component as well as its number average sequence length. Irrespective of composition, all the copolymers have good solubility in chloroform with glass transition temperature much below room temperature, implying good flexibility of the materials. The incorporation of PDO component could significantly increase the water wettability of the copolymer surfaces and thereby accelerate the degradation rate of the materials. In conclusion, flexible biodegradable polymers with adjustable degradation and crystalline properties were acquired by random copolymerization of CL and PDO, which are expected to use in tissue engineering and drug delivery fields. © 2013 Wiley Periodicals, Inc. J. Appl. Polym. Sci. 130: 2978–2986, 2013

INTRODUCTION

Aliphatic polyesters, with outstanding biodegradability, bioabsorbability, and biocompatibility, have attracted great interest from researchers in recent decades. The most notable examples include poly(D,L-lactide) (PDLLA), poly(L-lactide) (PLLA), poly(glycolide) (PGA) and their copolymers, and remarkable achievement has been made for their commercial use as implanted devices and drug delivery carriers.[1–5] Although these commercially available polyesters have good biodegradability and biocompatibility, their intrinsic brittleness is a problem when the material is applied to contact with soft tissues. To meet the demands for better healthy and improved clinical handling property, there is a requirement to develop materials with enough flexibility but also degraded in a reasonable time. So copolymerization or blending has been applied to create new biodegradable materials with attractive properties and potentialities.[6–13] However, the endeavor to increase material flexibility by the introduction of flexible unit or component often gave rise to much decreased degradation rate. Thus, it is still a very challenging work to acquire suitable biodegradable polymers with good flexibility and appropriate degradation rate.

Poly(*p*-dioxanone) (PPDO) is a biodegradable polymer with special ester–ether unit structure and was approved by FDA to fabricate surgical suture. The co-existence of ester and ether bonds in each unit of PPDO backbone endows it with not only good degradability but also high flexibility and good tensile strength. The adsorption period of PPDO material in human body is about 6 months that is similar to PGA but quite faster than PDLLA and PLLA.[14] Further, different from the brittle nature of PLA and PGA, PPDO is very tough with a maximum elongation to break at about 600%.[15] Thus, it is now considered as a very attractive material to make bioresorbable medical devices with great commercial value. However, PPDO did not become the research focus of polyesters for quite a long period. One reason is that the monomer PDO was not commercially available in the past. The second reason is that the activity of the PDO monomer is comparatively low, and most catalysts that have been mentioned in the available information are not effective enough to produce the polymer at reasonable cost.[16] Furthermore, a significant problem with PPDO used in drug delivery and tissue engineering fields is its limited solubility in common organic solvents such as methylene chloride or acetone,
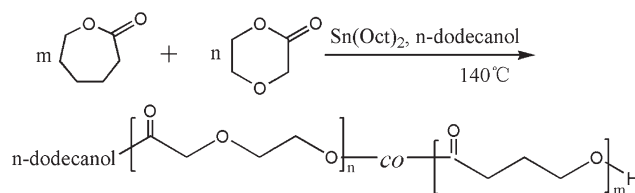
Scheme 1. Synthesis of P(CL-co-PDO) random copolymers.

because many of the techniques for making the controlled release formulations or scaffolds require the polymer to be dissolved in a slightly polar solvent. Fortunately, the synthetic method of producing PDO monomer has been simplified greatly, and studies on PDO copolymerization have made rapid development in recent years.

Poly(ε-caprolactone) is also well known for its non-toxicity, biocompatibility, biodegradability, and permeability, and these characteristics make it a good candidate for drug delivery. However, the rather hydrophobic nature of PCL undermines its biodegradability and impedes practical applications. In contrast, PPDO has fast degradation rate, excellent flexibility, pliability, and good tensile strength. Therefore, copolymerization between the two corresponding monomers is an effective way to combine excellent properties of individual components and improve the unsatisfied properties of each homopolymer. In recent years, block copolymerization of these two monomers has been reported by some researchers.[11,17–20] Raquez et al. synthesized the semicrystalline poly(PDO-b-CL) block copolymers, which displayed two well-separated melting temperatures at ca. 55 and 102°C for PCL and PPDO sequences, respectively.[20] However, as we understand, the study about random copolymerization of CL and PDO and properties of the copolymerized materials was very few.[21,22] As compared with block copolymerization, random copolymerization could tune the unit sequence length more precisely by the change of composition or polymerization conditions, allowing production of materials with a wide spectrum of properties.

In this article, P(CL-co-PDO) random copolymers with different compositions were synthesized by the change of CL/PDO feed ratio under fixed polymerization conditions. The reaction scheme can be found in Scheme 1. The number average sequence lengths for CL and PDO units were analyzed by

^{1}H-NMR data. The correlation between copolymer composition and microstructure with various properties such as crystallinity, thermal properties, surface properties, and degradation behavior will be presented.

EXPERIMENTAL

Materials
CL (Aldrich, 99%) was dried over CaH_2 at room temperature for 48 h and distilled under reduced pressure. PDO was synthesized by well established procedures from ethylene glycol and chloroacetic acid and purified by repeated recrystallization from ethyl acetate to achieve a purity of over 99.5%.[23] 1-Dodecanol and stannous octoate [$Sn(Oct)_2$] were both purchased from Aldrich and used directly without further purification. Other reagents were used as received.

Synthesis of P(CL-*co*-PDO) Random Copolymers
The P(CL-*co*-PDO) copolymers were synthesized in bulk using various CL/PDO comonomer mole feed ratios (Table I). The $Sn(Oct)_2$ and 1-dodecanol concentrations were both kept constant at 0.1 wt % relative to the total monomer concentration. All reagents were weighed into a round-bottomed flask, purged with argon three times, and then freeze-dried under high vacuum for 12 h. Then the copolymerization was carried out in an oven at 140°C for 20 h (Scheme 1).

The resultant copolymers were finally purified twice by dissolving into chloroform and then precipitated in a 10-folds excess of ethanol. The purified copolymers were dried under vacuum at 80°C for 24 h.

Preparation of Copolymer Films
The copolymer thick films with thicknesses of 0.2–0.4 mm were prepared by casting solutions of the copolymers in chloroform at a concentration of 10 wt % onto the surfaces of aluminum foil. The films were dried at 60°C under atmospheric pressure for 24 h and then further dried under vacuum at room temperature for another 24 h. The thick copolymer films were stored in a desiccator for further degradation experiments, and DSC, WAXD, and POM measurements

The copolymer thin films with thicknesses of 100 nm used for the investigation of surface properties were spin-cast from copolymer solutions (2 wt % in chloroform) at 3000 rpm for three minutes on round glass disks (0.7 mm × Ø 14 mm). The

Table I. Chemical Characterization and Molecular Weights of P(CL-*co*-PDO) Random Copolymers

Copolymers	f_{PDO}^a mol %	F_{PDO}^b mol %	L_{CL}	L_{PDO}	R	$[\eta]^c$ (dl/g)	$M_w^d \times 10^4$	$Đ^d$
P(CL90-*co*-PDO10)	10	7.7	15.5	1.23	0.84	1.35	9.18	2.06
P(CL80-*co*-PDO20)	20	17.1	5.28	1.10	1.10	0.88	7.96	1.90
P(CL70-*co*-PDO30)	30	26.2	3.22	1.15	1.18	0.74	6.52	2.05
P(CL50-*co*-PDO50)	50	42.9	2.06	1.54	1.13	0.54	4.90	1.81
P(CL30-*co*-PDO70)	70	61.3	1.46	2.31	1.12	0.50	4.56	1.78
P(CL20-*co*-PDO80)	80	73.0	1.27	3.43	1.08	0.38	3.24	1.69
P(CL10-*co*-PDO90)	90	82.6	1.20	5.70	1.01	0.29	-	-

[a] Amount of L-lactide in the feedstock, [b] Amount of L-lactide units in the polymer chain, as determined by ^{1}H NMR, [c] $[\eta]$ was measured in chloroform at 25°C, [d] Samples were recorded in THF versus PS standards.

glass disks were previously soaked in a potassium dichromate/sulfuric acid solution for 48 h and then rinsed thoroughly with distilled water and acetone. The spin-cast films were dried at room temperature for 48 h and stored in a desiccator for further surface properties studies, such as AFM and contact angle measurements.

In Vitro Degradation

Degradations experiments for P(CL-*co*-PDO) copolymers were carried out in PBS medium (pH 7.4). P(CL-*co*-PDO) samples were immersed in 6 mL of buffer solution in screw capped tubes and placed in an orbital shaker bath which was maintained at 37°C. After a particular time interval, the tubes were taken out of the bath, and the samples in triplicate were recovered, washed several times with distilled water and vacuum-dried before being subjected to other analyses.

Methods

The gel permeation chromatography (GPC) measurements were performed on a Waters 1515 GPC system with a Waters 2414 refractive-index detector (America) using THF as eluent and polystyrene as standards.

The Intrinsic viscosities [η] of the resulting polymers were measured in chloroform solutions using an Ubbelohde viscosimeter thermostated at 25°C, and all of the solutions were filtered before measurement.

The proton nuclear magnetic resonance (^{1}H-NMR) spectra were recorded on a 300 MHz ^{1}H-NMR spectrometer (Bruker AV-300), using tetramethylsilane as an internal reference and CDCl$_3$ as the solvent.

The differential scanning calorimetry (DSC) analysis was performed on a TA Q20 instrument to study the thermal behavior of the synthesized copolymers over a temperature range from −80 to 140°C at heating and cooling rates of 10°C/min.

Wide-angle X-ray diffractions (WAXD) experiments for the film samples were performed on an X-ray diffractometer (Philips X'Pert X-ray diffractometer) with Cu $K\alpha$ radiation at room temperature with a scan rate of 2°/min scanning from 10° to 35°.

Surface morphology characterization was done by using an AFM in the tapping mode (Nanoscope III) equipped with a standard Si tip and operated at a scan size of 10 × 10 μm^2 in air at room temperature.

Polarized optical microscopy (POM) studies were carried out with a ECLIPSE LV100POL microscope (Nikon, Japan). The specimens were heated to 140°C on a hot stage for 3 min, and then quickly cooled to crystallization temperature.

Contact angle analysis was performed on a KRÜSS DSA100. Each experiment included multiple immersions to ensure consistent and reproducible data. For all data reported herein we required at least three identical immersions in succession.

RESULTS AND DISCUSSION

Synthesis and Microstructure Analysis of P(CL-*co*-PDO) Random Copolymers

A series of random copolymers of CL and PDO were synthesized in bulk using Sn(Oct)$_2$ and 1-dodecanol as the initiating system (Scheme 1). Table I shows the ^{1}H-NMR and GPC data of the copolymers with various compositions. In this article, a copolymer notation such as P(CL70-*co*-PDO30) means that the initial comonomer feed consisted of 70 mol % CL and 30 mol % PDO. It is observed in Table I that the mole fractions of PDO monomer (f_{PDO} %) in the initial comonomer feeds are higher than those actual values (F_{PDO} %) in the copolymers determined by ^{1}H-NMR. This is due to the unzipping depolymerization of PDO unit from the chain end occurring during the copolymerization process.[24] As a consequence, large amounts of residual PDO monomer are formed in equilibrium with the copolymer chains.

The chain microstructure and randomizing degree of the copolymers was studied by ^{1}H-NMR. Figure 1 shows representative ^{1}H-NMR spectra of the P(CL70-*co*-PDO30) copolymer. The peaks positioned at 4.35–4.40 ppm [Figure 1(c)] and 2.25–2.33 [Figure 1(d)] represent the ^{1}H-NMR resonances of methylene groups in the unit of the PDO-PDO* and CL-$CL^\star$ sequence. It is worth to note that additional peaks at positions 4.25–4.30 ppm [Figure 1(c′)] and 2.33–2.39 [Figure 1(d′)] also emerge and correspond to the resonances of methylene group in the unit of CL-PDO* and PDO-$CL^\star$ sequence, respectively. Very recent pieces of evidence suggest that the actual initiator for the ROP of lactides or lactones by Sn(Oct)$_2$ is formed *in situ* in the interchange reactions between Sn(Oct)$_2$ and hydroxyl containing compounds present in the reaction medium.[25] Elementary chain-growth reaction consists of the concerted monomer insertion into the alkoxide oxygen–metal bond followed by the acyl–oxygen bond scission and reformation of the alkoxide species. The major side reactions in ROP of lactones or lactides are chain transfers with chain rupture, also called inter- or intramolecular transesterification reaction. They contribute to redistribution of the sequences along the polymer chains leading to changes in the chain structure and the lengths of microblocks.

The intensity of peak c is close to that of peak c′, implying a random structure generated. By comparison of peak intensity representing PDO-PDO* and CL-PDO* sequences and that representing CL-$CL^\star$ and PDO-$CL^\star$ sequences, it is possible to calculate the experimental number-average lengths of CL and PDO blocks, L_{CL} and L_{PDO}, respectively, in the copolymers according to the following equations:

$$L_{PDO} = I_{PDO-PDO*}/I_{CL-PDO*} + 1 \qquad (1)$$

$$L_{CL} = I_{CL-CL*}/I_{PDO-CL*} + 1 \qquad (2)$$

where $I_{PDO-PDO*}$ and $I_{CL-PDO*}$ indicate the peak intensity of PDO-PDO* and CL-PDO* sequences of the copolymer calculated from ^{1}H-NMR, and $I_{CL-CL^\star}$ and $I_{PDO-CL^\star}$ represent the peak intensity of CL-$CL^\star$ and PDO-$CL^\star$ sequences of the copolymer determined by ^{1}H-NMR.

Copolymer randomness was evaluated by determining the sequence distribution in each copolymer. Therefore, the degree of randomness (R) of the copolymer chains can be calculated from the equation below:

$$R = 100/L_{PDO} + 100/L_{CL} \qquad (3)$$

The coefficient R is equal to 100 for completely random chains. From Table I, it is observed that the experimental number-

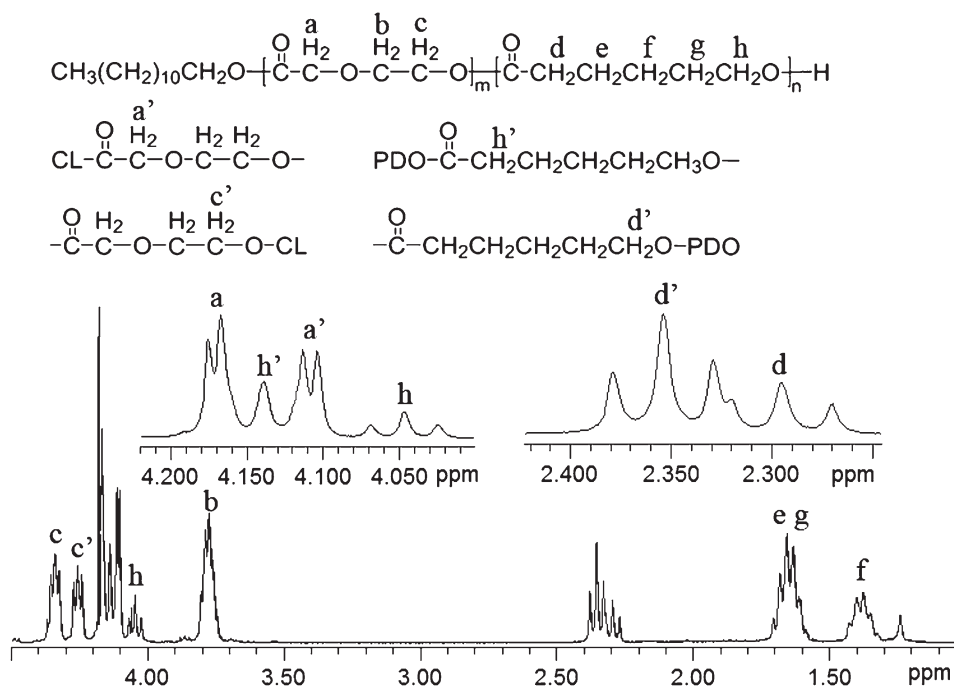**Figure 1.** ^{1}H-NMR spectra of P(CL30-*co*-PDO70) random copolymer.

average block length of PDO sequence increases with increasing PDO content in the copolymers. The R values are basically in the range of 100–114, which are close to 100 for completely random copolymer, indicating the formation of random copolymers.

The weight molecular weights and polydispersity indexes (M_w and Đ) of the synthesized copolymers are also summarized in Table I. The P(CL10-*co*-PDO90) sample could not be dissolved into THF, and its M_w and Đ data were not available. There is no evidence to indicate that the copolymer products contained any PCL or PPDO homopolymeric fractions from the GPC chromatograms. Further, the microstructure analysis by ^{1}H-NMR also ruled out the existence of PCL and PPDO. From Table I, we can also see that the Mw of the copolymers decreased as the content of PDO increased in the copolymer. The unzipping depolymerization of PDO and more residual water content in PDO monomer may be the reason.

The solubilities of the copolymers were tested using chloroform as the solvent, which is one of the most popular solvents to process biodegradable polymers. Irrespective of composition, all the copolymers could dissolve into chloroform very easily with unlimited solubility, indicating their potential applications in drug delivery and tissue engineering fields.

Thermal Properties and Crystallinity of P(CL-*co*-PDO) Random Copolymers

DSC was used to study the influences of the chemical composition and microstructure on thermal properties of P(CL-*co*-PDO) copolymers. The DSC first heating curves (performed at 10°C) of the copolymers are shown in Figure 2(A). The P(CL10-*co*-PDO90) and P(CL20-*co*-PDO80) copolymers show

obvious melting peak, corresponding to the melting of crystals formed by PDO blocks. When the PDO content is in the range of 70–50 mol %, the copolymers loss the ability to crystallize and exist in an amorphous state. When the CL component is dominating in the copolymers, obvious melting peak, corresponding to the melting of crystals formed by CL blocks, appears for the P(CL70-*co*-PDO30), P(CL80-*co*-PDO20), and P(CL90-*co*-PDO10) copolymers. Figure 3 summarizes the relation between the crystallinity with composition and microstructure of the copolymers. It is seen that although CL and PDO are both crystalline components, there is no case of composition that two crystalline phases could coexist. For the crystalline copolymers, the low limit of number average block length for crystallization is 3.22 for L_{CL} and 3.38 for L_{PDO}, respectively.

Figure 2(B) shows DSC subsequent cooling scans of the random copolymers. It can be seen that the copolymers with CL as the major component show obvious crystallization peaks. And the crystallization temperature decreased as the CL content decreased in the copolymers. However, for other compositional copolymers, even that containing 90 mol PDO, there is no detectable crystallization peak. This could be ascribed to the weak crystallization ability of PDO blocks in the copolymers compared to CL blocks. After the cooling, the copolymer was heated again from −80 to 200°C at a rate of 10°C/min to detect the glass transition temperatures [Figure 2(C)]. From Figure 4, it is observed that the glass transition temperature of the copolymers increases linearly with increasing PDO content in the copolymers. All the T_g values lies in between the extreme values for PCL (−60°C) and PPDO (−10°C) homopolymers, and are much lower than room temperature, indicating the good flexibility of the materials.
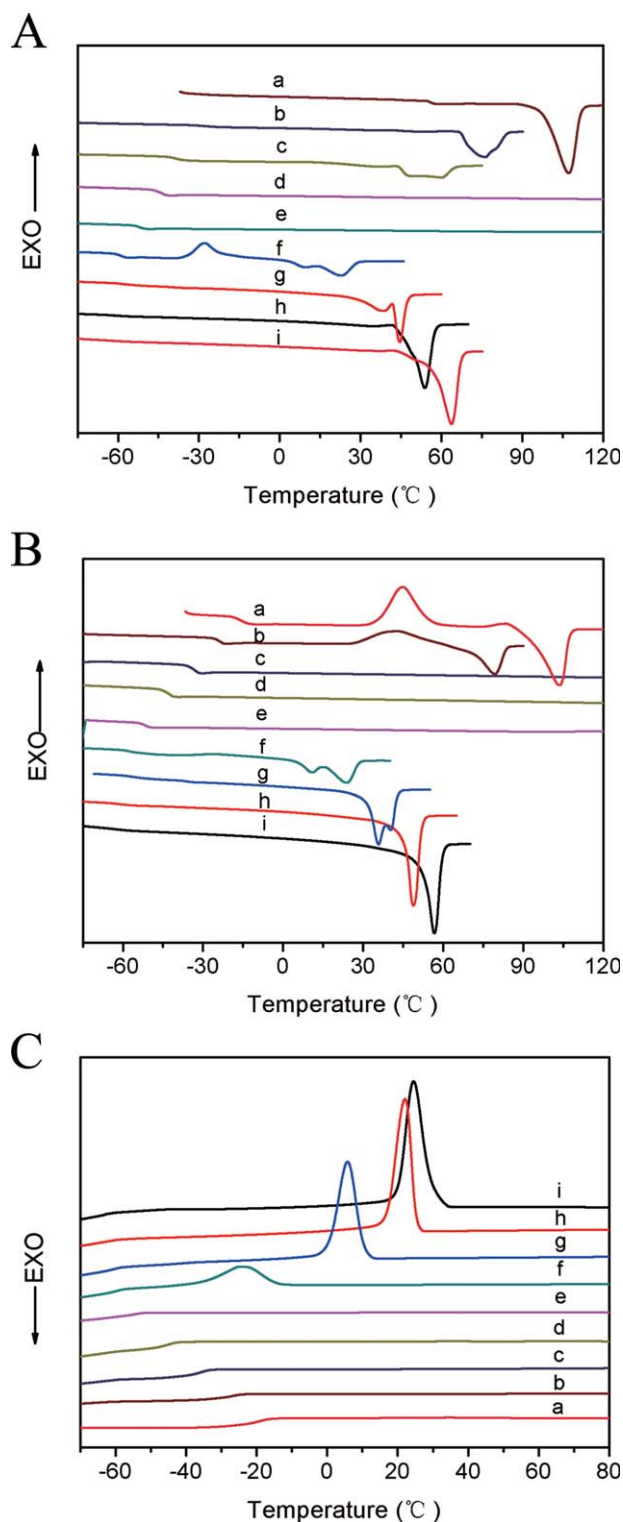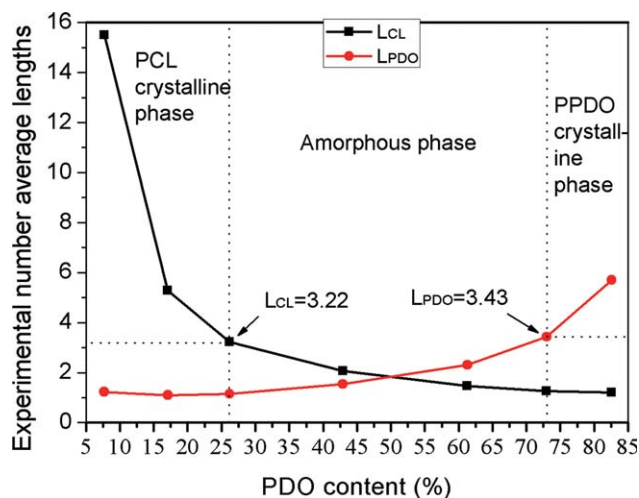
Figure 3. Correlation of chemical composition and microstructure with the crystallizability of the copolymers. [Color figure can be viewed in the online issue, which is available at wileyonlinelibrary.com.]

The degree of crystallinity (X_c) of the PDO and CL units for the copolymers can be calculated according to the following relation:

$$X_c = H_f / (w \times H_{f,100})$$

where $\Delta H_{f100\%}$ and ΔH_f indicate the heats of fusion for a 100% crystalline PDO or CL homopolymer and the copolymer, respectively, w is the weight fraction of PDO or CL units in the copolymer. To calculate $X_{c,PDO}$ and $X_{c,CL}$, the literature value of $\Delta H_{f100\%}$ = 14.4 kJ/mol and 142 J/g were used, respectively,[26,27] and the results are shown in Figure 5. It is shown that the degree of crystallinity of $X_{c,CL}$ and $X_{c,PDO}$ decreased as the content of CL and PDO decreased, respectively. From Figure 3, the crystallinity of the copolymers could be directly correlated to the number average sequence length of the crystalline component, which otherwise could be tuned by the change of composition.

The crystalline structures of the copolymers were further investigated by WXRD (Figure 6). In the spectra, the appearance of two Bragg peaks at 21.32° and 23.69° [Figure 6(A–C)]
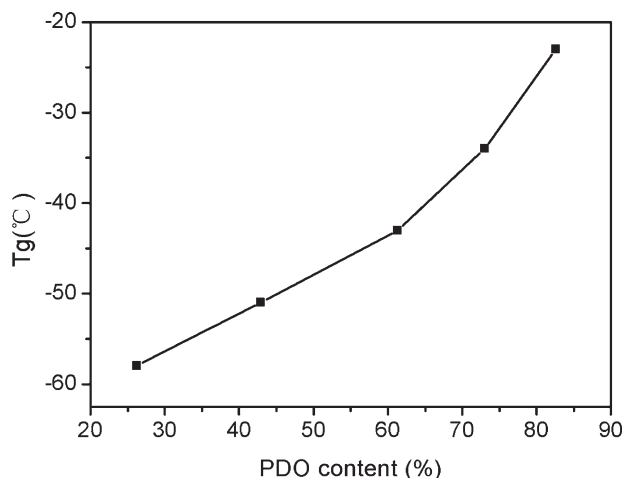

Figure 4. Change of glass transition temperature (T_g) of the copolymers with PDO content in the copolymers.

Figure 2. DSC first heating scans (A), subsequent cooling scans (B) and second heating scans (C) of the copolymer samples: (a) PPDO; (b) P(CL10-*co*-PDO90); (c) P(CL20-*co*-PDO80); (d) P(CL30-*co*-PDO70); (e) P(CL50-*co*-PDO50); (f) P(CL70-*co*-PDO30); (g) P(CL80-*co*-PDO20); (h) P(CL90-*co*-PDO10); (i) PCL. [Color figure can be viewed in the online issue, which is available at wileyonlinelibrary.com.]
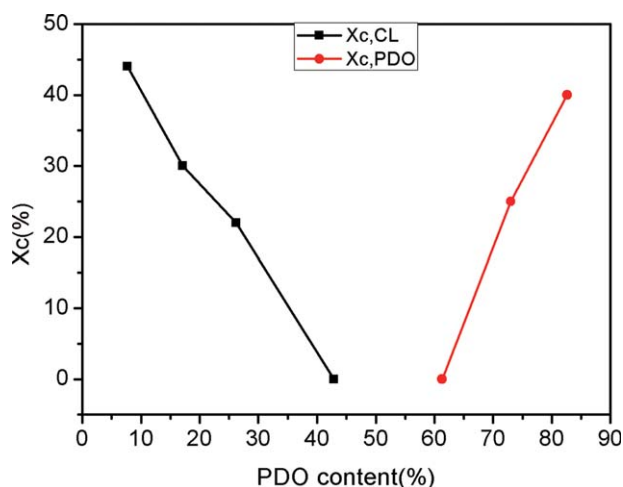
Figure 5. Change of crystallinity (X_c) of the copolymers with PDO content in the copolymers acquired from the first heating curves. [Color figure can be viewed in the online issue, which is available at wileyonlinelibrary.com.]

correspond to the characteristic peaks for PCL homopolymer and confirm the crystalline phase derived from the PCL component.[28] And, the appearance of two Bragg peaks at 21.95° and 23.90° [Figure 6(D–F)] correspond to the characteristic peaks for PPDO homopolymer and confirm the crystalline phase derived from the PPDO component.[7] This result shows that there is only one crystallization phase for each crystalline copolymer. By comparison of the area representing the crystalline and the amorphous regions in the WXRD patterns, the crystallinities could be estimated and show agreement with those data from DSC analysis.

Surface Properties of P(CL-co-PDO) Random Copolymers

The surface morphology and crystalline structures of the copolymer films were characterized by atomic force microscopy (Figure 7). For the crystalline copolymers with higher L_{CL}, such as P(CL90-co-PDO10) and P(CL80-co-PDO20) samples [Figure 7(A,B)], the surfaces are quite rough and show typical spherulitic domains that spread over the whole film surfaces. Well-defined and clear boundaries between the spherulites are observed. In contrast to the spherulitic structure, the crystalline copolymer with a predominant PDO content, such as P(CL10-co-PDO90) sample [Figure 7(E)], shows fibrous crystalline structure. This difference in crystalline morphology may be due to the decreased crystallizability of PDO component as compared to CL component, which was exhibited much significantly when the crystals grew in a substrate-confined environment (100 nm thickness). For the composition intermediate copolymers with low crystallinity, such as P(CL70-co-PDO30) and P(CL20-co-PDO80) [Figure 7(C,D)], the crystalline structure could not occupy the whole sample and appears as dispersed domains in a continuous amorphous matrix. When correlating the chemical microstructure with crystalline morphology of the copolymers, it is concluded that the low limit of number average sequence length for the crystalline domains to fill over the whole samples is 5.28 for L_{CL} and 5.85 for L_{PDO}, respectively.

Figure 8 illustrates the crystalline morphologies of the copolymer samples observed by POM. It can be seen that the P(CL10-co-PDO90) sample shows perfect large spherulitic morphology with typical maltese cross patterns clearly observed [Figure 8(C)]. This indicates that that PDO blocks were able to crystallize with a well-defined spherulitic morphology even in the presence of CL units. For P(CL90-co-PDO10) and P(CL80-co-PDO20) copolymers, the spherulites are coarser and smaller with unclear boundaries and disrupted concentric rings observed [Figure 8(A,B)], suggesting that the CL crystalline phase had less regularity even the copolymers containing a low PDO content.

The water wettability of the copolymer surfaces were assessed using static contact angle analysis because this parameter is important for hydrolytic degradation of the copolymers. The static contact angles of all the copolymers examined in this study are shown in Figure 9. The resultant static contact angle was observed to statistically decrease with increasing PDO content. In all cases, the presence of PDO led to a significant improvement in material hydrophilicity. This was because of the good compatibility of PDO segments with water due to the presence of ether bonds. It is expected that the copolymers with more hydrophilic content exhibited a much faster degradation rate when subjected to hydrolytic degradation *in vivo*.

Degradation Properties of P(CL-co-PDO) Random Copolymers

Determining the weight loss and the molecular weight change of the samples during exposure to the hydrolysis medium is simple indication for tracing the progress of hydrolytic degradation. Figure 10 shows the percentage of retained weight of the samples as a function of degradation time. It can be seen from Figure 10, the weight loss of the samples with CL as the major component is almost unchangeable during the 12 weeks' degradation time. However for the copolymers with a predominant PDO content, a significant decrease of weight loss with
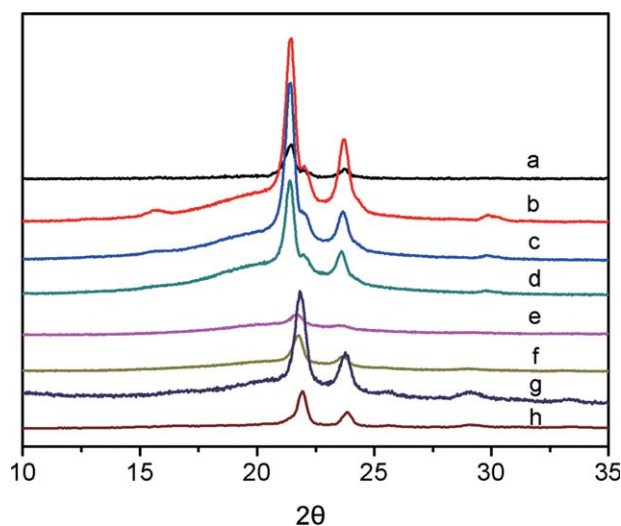

Figure 6. WAXD spectra of the copolymers: (a) PCL; (b) P(CL90-co-PDO10); (c) P(CL80-co-PDO20); (d) P(CL70-co-PDO30); (e) P(CL30-co-PDO70); (f) P(CL20-co-PDO80); (g) P(CL10-co-PDO90); (h) PPDO. [Color figure can be viewed in the online issue, which is available at wileyonlinelibrary.com.]
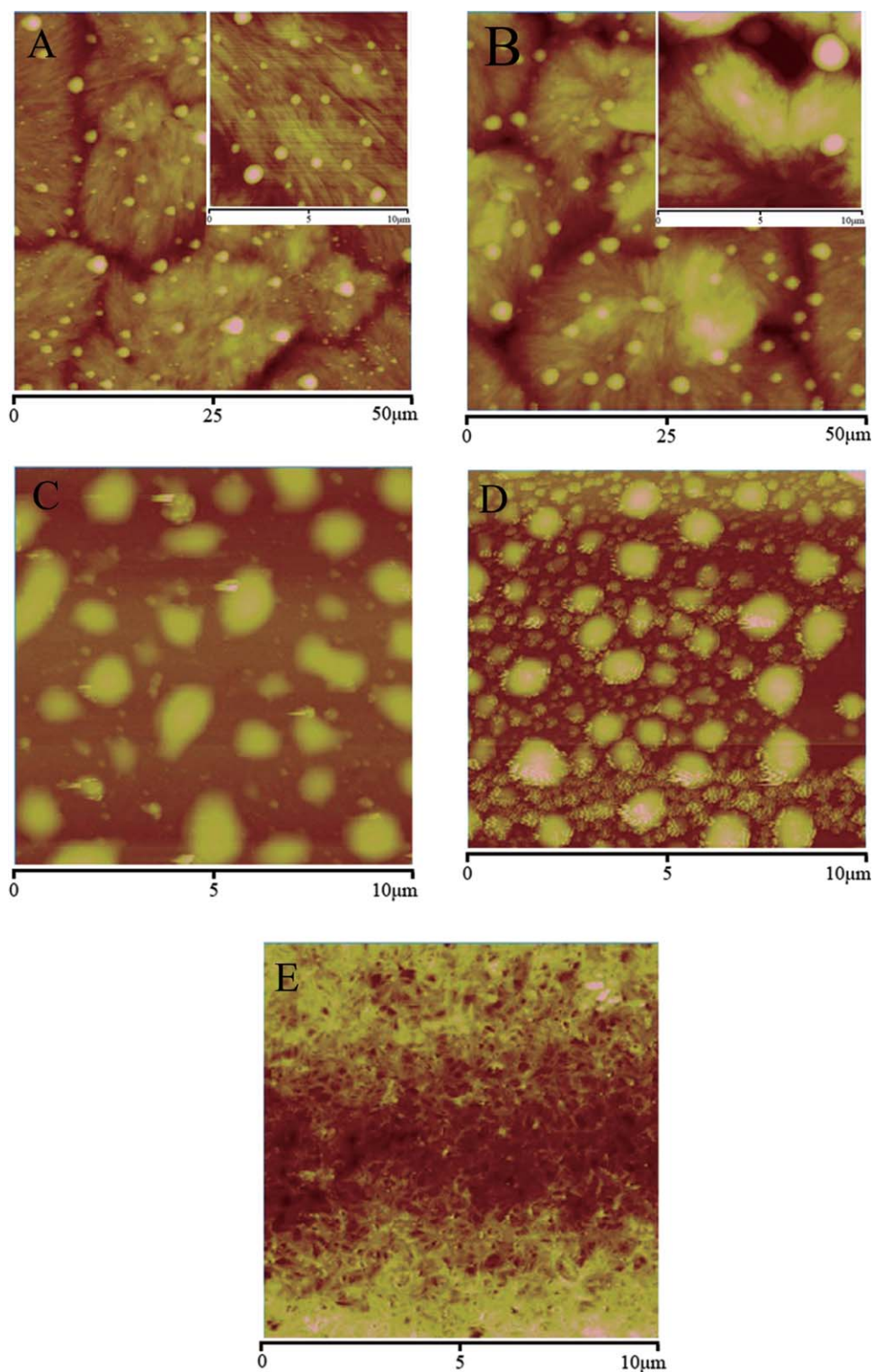
Figure 7. AFM micrographs of the copolymer thin-film surfaces: (A) P(CL90-*co*-PDO10); (B) P(CL80-*co*-PDO20); (C) P(CL70-*co*-PDO30); (D) P(CL20-*co*-PDO80); (E) P(CL10-*co*-PDO90). [Color figure can be viewed in the online issue, which is available at wileyonlinelibrary.com.]

degradation time is observed. And the degradation of the samples was directly correlated with copolymer composition. These facts indicate that the weight loss of P(CL-*co*-PDO) random copolymers was mainly determined by the major component.

The addition of slow degradable CL units into PPDO at a low content could produce novel flexible materials with improved solubility and decreased crystallinity, but will not sacrifice too much the fast degradation rate for PPDO.
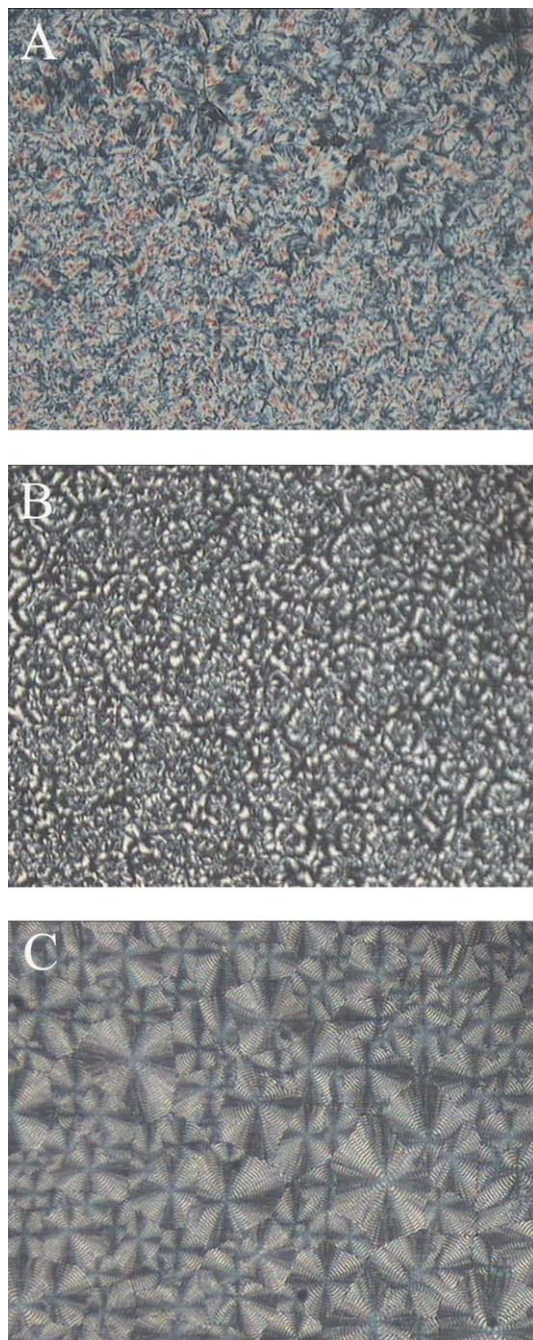
Figure 8. POM micrographs for non-isothermally crystallized copolymer samples: (A) P(CL90-*co*-PDO10); (B) P(CL80-*co*-PDO20); (C) P(CL10-*co*-PDO90). [Color figure can be viewed in the online issue, which is available at wileyonlinelibrary.com.]

Figure 11 shows the change in molecular weight of the copolymers with degradation time. For all the copolymer samples, the molecular weight decreases obviously with the degradation time. Specifically for the samples with CL as the major component, the decrease of molecular weight during the first 2 weeks appears more sharply with increasing PDO content in the copolymers. This trend is in accordance with the change of number average sequence length of PDO units. Since CL–CL linkages hydrolyzed much slowly due to the hydrophobic
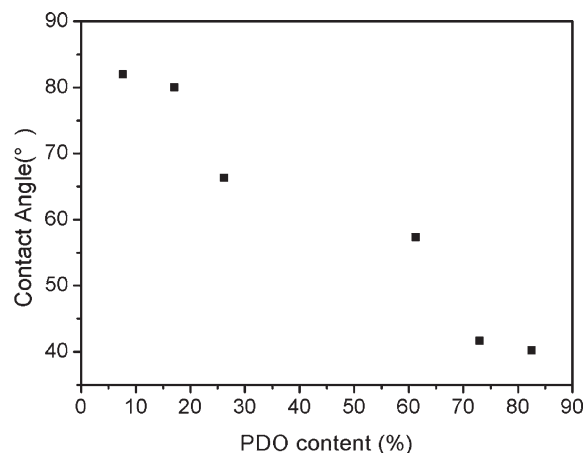

Figure 9. Change of water contact angle with PDO content in the copolymers measured on the thin-film surfaces.
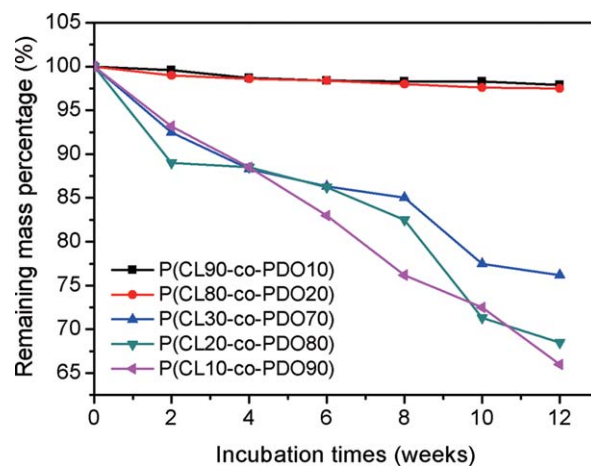

Figure 10. Remaining mass percentages of the copolymer thick films incubated in PBS (pH = 7.41) at 37°C. [Color figure can be viewed in the online issue, which is available at wileyonlinelibrary.com.]
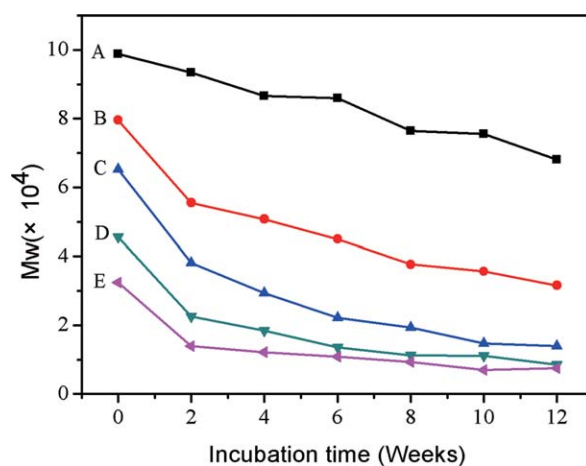

Figure 11. Change of molecular weight of the copolymer thick films incubated in PBS (pH = 7.41) at 37°C: (A) P(CL90-*co*-PDO10); (B) P(CL80-*co*-PDO20); (C) P(CL70-*co*-PDO30); (D) P(CL30-*co*-PDO70); (E) P(CL20-*co*-PDO80). [Color figure can be viewed in the online issue, which is available at wileyonlinelibrary.com.]

nature, the above trend could be ascribed to the cleavage of PDO–PDO linkages in the copolymer chains that were more accessible to hydrolysis.

CONCLUSIONS

A series of P(CL-*co*-PDO) copolymers with different compositions were synthesized by bulk ring-opening polymerization of CL and PDO monomers using $Sn(Oct)_2/n$-dodecanol as the initiating system. The chain microstructure and randomizing degree of the copolymers were analyzed by ^{1}H-NMR, which revealed the random copolymerization mechanism. For the dual-crystalline solvent-cast samples, there is no case of composition that two crystalline phases could coexist. Both the crystallinity and crystalline morphology is dependent on the major component as well as its number average sequence length. The presence of CL units could improve the solubility of the copolymers, which could dissolve into chloroform very easily with high concentration. The copolymers show composition-dependent T_g values, which are much lower than room temperature and implies the flexibility of the copolymers. The incorporation of PDO component could enhance the hydrolytic behavior of the copolymers, and the copolymers with PDO as the major component have much faster degradation rates as compared with those containing a predominant CL content. In conclusion, P(CL-*co*-PDO) random copolymers are promising biodegradable candidates with potential applications in drug delivery and tissue engineering fields, due to their good flexibility, and solubility, as well as adjustable degradation properties.

ACKNOWLEDGMENTS

REFERENCES

1. Rokkanen, P. U.; Böstman, O.; Hirvensalo, E.; Mäkelä, E. A.; Partio, E. K.; Pätiälä, H.; Vainionpää, S.; Vihtonen, K.; Törmälä, P. *Biomaterials* **2000**, *21*, 2607.

2. Hao, J. Y.; Keller, T.; Cai, K. Y.; Klem, E.; Bossert, J.; Jandt, K. D. *Adv. Eng. Mater.* **2008**, *10*, B23.

3. Pack, J. W.; Kim, S. H.; Cho, I. W.; Park, S. Y.; Kim, Y. H. *J. Polym. Sci. Part A: Polym. Chem.* **2002**, *40*, 544.

4. Choi, E. J.; Park, J. K.; Chang, H. N. *J. Polym. Sci. Part B: Polym. Phys.* **1994**, *32*, 2481.

5. Bero, M.; Kusperczyk, J. *Macromol. Chem. Phys.* **1996**, *197*, 3251.

6. Wang, T. Q.; Ding, J.; Zhao, X. L.; Liu, Y.; Hao, J. Y. *J. Polym. Environ.* **2012**, *20*, 157.

7. Zhao, H. Z.; Wang, T. Q.; Zhao, X. L.; Liu, Y.; Hao, J. Y. *J. Polym. Environ.* **2012**. DOI: 10.1007/s10924-012-0526-2.

8. Lendlein, A.; Zotzman, J.; Feng, Y. K.; Alteheld, A.; Kelch, S. *Biomacromolecules* **2009**, *10*, 975.

9. Zhou, Z. X.; Wang, X. L.; Wang, Y. Z.; Yang, K. K.; Chen, S. C.; Wu, G.; Li, J. *Polym. Int.* **2006**, *55*, 383.

10. Zeng, J. B.; Zhu, Q. Y.; Li, Y. D.; Qiu, Z. C.; Wang, Y. Z. *J. Phys. Chem. B.* **2010**, *114*, 14827.

11. Hong, J. T.; Cho, N. S.; Yoon, H. S.; Lee, D. H.; Kim, W. G. *J. Polym. Sci. Part A: Polym. Chem.* **2005**, *43*, 2790.

12. Wu, G.; Chen, S. C.; Zhan, Q.; Wang, Y. Z. *Macromolecules* **2011**, *44*, 999.

13. Wang, T. Q.; Hao, J. Y.; Liu, Y.; Gu, Z. W. *RSC Adv.* **2012**, *2*, 10365.

14. Redin, T.; Finne-Wilstrand, A.; Mathisen, T.; Albertson, A. C. *J. Polym. Sci. Part A: Polym. Chem.* **2007**, *45*, 5552.

15. Doddi, N.; Versfelt, C. C.; Wasserman, D. US Pat. 4,032,988, **1997**.

16. Yang, K. K.; Wang, X. L.; Wang, Y. Z. *Polym. Rev.* **2002**, *42*, 373.

17. Hong, J. T.; Cho, N. S.; Yoon, H. S.; Kim, T. H.; Koh, M. S.; Kim, W. G. *J. Appl. Polym. Sci.* **2006**, *102*, 737.

18. Tzoneva, R.; Weckwerth, C.; Seifert, B.; Behl, M.; Heuchel, M.; Tsoneva, I.; Lendlein, A. *J. Biomater. Sci. Part C: Polym. Ed.* **2011**, *22*, 2205.

19. Albuerne, J.; Márquez, L.; Müller, A. J.; Raquez, J. M.; Castelletto, V.; Hamley, I. W. *Macromolecules* **2006**, *36*, 1633.

20. Müller, A. J.; Albuerne, J.; Esteves, L. M.; Marquez, L.; Raquez, J. M.; Degée, P.; Dubois, P.; Collins, S.; Hamley, I. W. *Macromol. Symp.* **2004**, *215*, 369.

21. Chen, R.; Hao, J. Y.; Xiong, C. D.; Deng, X. M. *Chinese Chem. Lett.* **2010**, *21*, 249.

22. Bezwada, R. S.; Shalaby, S. W.; Erneta, M. US Pat. 5,047,048, **1991**.

23. Ying, J. US Pat. 5,391,707, **1995**.

24. Rodriguez-Galan, A.; Franco, L.; Puiggali, J. *J. Polym. Sci. Part A: Polym. Chem.* **2009**, *47*, 6758.

25. Peter, J. A.; Veld, I. V.; Esther, M. V.; Peter, V. W.; Jennie, H.; Pieter, J. D.; Feijen, J. *J. Polym. Sci. Part A: Polym. Chem.* **1997**, *35*, 219.

26. Wunderlich, B. Macromolecular Physics: Crystal Melting. Academic Press: New York, **1980**; Vol. 3, p 54.

27. Zhu, J.; Dong, X. T.; Wang, X. L.; Wang, Y. Z. *Carbohydr. Polym.* **2001**, 541.

28. Wang, K.; Li, W. W.; Gao, K. *J. Appl. Polym. Sci.* **2007**, *105*, 629.